Compressibility of stottite, FeGe(OH)₆: An octahedral framework with protonated O atoms

NANCY L. ROSS,[1,]* TRACEY D. CHAPLIN,[2] AND MARK D. WELCH[3]

[1]Department of Geological Sciences, Virginia Polytechnic Institute and State University, Blacksburg, Virginia 24061, U.S.A.
[2]Department of Geological Sciences, University College London, Gower Street, London WC1E 6BT, U.K.
[3]Department of Mineralogy, Natural History Museum, Cromwell Road, London SW7 5BD, U.K.

ABSTRACT

The evolution of the unit-cell parameters of stottite [FeGe(OH)$_6$], a compound with a tetragonal octahedral framework related to the perovskite structure, has been determined to a maximum pressure of 7.8 GPa by single-crystal X-ray diffraction at room temperature. Stottite does not exhibit any phase transitions in this pressure range. A fit of a third-order Birch-Murnaghan equation of state to the pressure-volume data yields values of $V_0 = 425.67(2)$ Å^3, $K_{T0} = 78.4(3)$ GPa and $K'_0 = 6.18(10)$. Analysis of the unit-cell parameter data shows that **c** is approximately 10% more compressible **a**. Compressional moduli for the axes are $K_{a0} = 81.3(3)$ GPa and $K'_{a0} = 6.4(1)$, $K_{c0} = 73.3(6)$ GPa and $K'_{c0} = 5.7(2)$. We relate these axial compressibilities to the structure of stottite, which, unlike related cubic protonated octahedral frameworks such as burtite [CaSn(OH)$_6$], is expected to have a highly anisotropic hydrogen-bonding topology: a high degree of hydrogen-bonded connectivity parallel to (001) and very little parallel to [001]. Enhanced hydrogen bonding within the (001) plane may stiffen the structure along <100>. We also make some provisional comparisons with structural and elasticity data for perovskites and show that the absence of a central, non-framework cation in the stottite structure allows octahedral tilts in excess of 40°. The stottite structure is much softer than any known oxide perovskite. The relative importance of an empty cavity site vs. the role of hydrogen bonding is likely to be a major issue in understanding the compressional behavior of protonated octahedral frameworks.

INTRODUCTION

The stottite group of minerals have structures comprising a framework of corner-linked octahedra in which all O atoms are protonated as hydroxyl groups. Nearly all stottite-group minerals, including burtite [CaSn(OH)$_6$], schoenfliesite [MgSn(OH)$_6$], wickmanite [MnSn(OH)$_6$], and natanite [FeSn(OH)$_6$], are cubic and belong to space group $Pn\overline{3}$ or $Pn3m$ (Moore and Smith 1967; Cohen-Addad 1968; Faust and Schaller 1971; Sonnet 1981; Basciano et al. 1998). However, stottite FeGe(OH)$_6$ and jeanbandyite Fe$^{3+}_{1-x}\square_x$Sn$_{1-y}\square_y$(OH)$_6$ are tetragonal and belong to space group $P4_2/n$ (Ross II et al. 1988; Kampf 1982). The aristotype structures related to these cubic and tetragonal structures have space groups $Im\overline{3}$ [e.g., Sc(OH)$_3$, Ga(OH)$_3$, In(OH)$_3$] and $I4/mmm$, respectively (O'Keeffe and Hyde 1977). Lowering of the space-group symmetries from those of the aristotypes arises from the ordering of the M^{2+} and M^{4+} octahedra in the framework so that they alternate with one another.

Strunz and Giglio (1961) performed the first single-crystal X-ray diffraction structure determination of stottite, which largely confirmed the original structure proposed by Zemann (1959). More recently, Ross II et al. (1988) refined the structure of stottite from three-dimensional single-crystal X-ray diffraction data and found a significant change in the location of O3 and an apparent lowering of symmetry from $P4_2/ncm$ to $P4_2/n$, $Z = 4$. The structure consists of alternating Fe(OH)$_6$ and Ge(OH)$_6$ octahedra in a three-dimensional, corner-sharing framework (Fig. 1). In terms of the Glazer notation for octahedral-tilt systems in perovskites (Glazer 1972), stottite corresponds to a $a^+a^+c^-$ tilt scheme with reversed senses of rotation of octahedra in alternate layers along [001] (Fig. 1). The average Fe-O distance is 2.159 Å, whereas the average Ge-O distance is 1.910 Å, in good agreement with interatomic distances determined by EXAFS (Bernstein and Waychunas 1987). The hydrogen positions in stottite are not yet determined, but they are expected to form across the short O-O distances ranging from 2.70 to 2.94 Å (Ross II et al. 1988).

The present study was undertaken as part of a wider project investigating the systematics of composition, hydrogen bonding, and compressibilities in protonated octahedral frameworks. Unlike perovskites, the cavity is empty, and so the effect of the absence of a non-framework cation upon physical properties can be studied. These minerals, with their extensive hydrogen bonding, also provide an excellent opportunity to study the effects of hydrogen bonding upon macroscopic properties such as compressibility. Here we report the first equation of state for stottite.

EXPERIMENTAL METHODS

The sample is from the germanium-rich horizon at Tsumeb, Namibia and was kindly donated by W. Pinch of Pittsford, New York State. The unit-cell parameters determined in this study, $a = 7.55041(9)$ Å, $c = 7.4664(4)$ Å, show excellent agreement
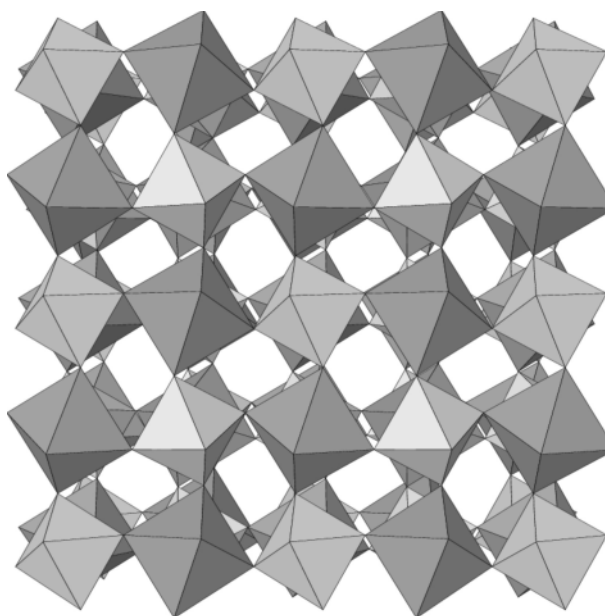
* E-mail: nross@vt.edu

with those of Strunz et al. (1958), a = 7.55 Å, c = 7.47 Å, and are slightly smaller than those reported by Ross II et al. (1988), a = 7.594(4) Å, c = 7.488(6) Å.

A single crystal suitable for high-pressure study was initially chosen on the basis of optical quality and then diffraction quality. The high-pressure measurements were performed with a BGI-design diamond-anvil cell (Allan et al. 1996) using T301 steel as a gasket. The stottite crystal was loaded into the diamond-anvil cell together with a ruby chip for approximate pressure measurements and a quartz crystal as an internal diffraction pressure standard. A 4:1 mixture of methanol:ethanol was used as the pressure medium. The constant widths of the diffraction peaks at all pressures indicated that this pressure medium remained hydrostatic up to the highest pressure achieved, 7.817 GPa. Diffraction measurements were performed with a Huber four-circle diffractometer. Full details of the instrument and the peak-centering algorithms are provided by Angel et al. (1997, 2000). Unit-cell parameters were determined at each pressure from a least-squares fit to the corrected setting angles of 18–20 reflections obtained by the eight-position centering method (King and Finger 1979). The unconstrained unit-cell parameters showed no significant deviation between a and b, and the angles show no significant deviation from 90°, indicating that the structure remains tetragonal over the pressure range of our data. The values of symmetry-constrained unit-cell parameters obtained by vector-least-squares (Ralph and Finger 1982) are reported in Table 1. Pressures were determined from the unit-cell volumes of the quartz crystal in the diamond anvil cell, using the equation of state reported by Angel et al. (1997). Equation of state parameters for stottite were obtained by a weighted-least-squares fit (Angel 2000) of the Birch-Murnaghan 3rd-order equation (Birch 1947) to the pressure-volume data. Weights for each datum were calculated by the effective variance method (Orear 1982) from the e.s.d. in the unit-cell volume combined with the uncertainty in pressure corresponding to the e.s.d. of the unit-cell volume of the quartz pressure standard.

RESULTS

Both the volume and cell parameters of stottite decrease smoothly with increasing pressure, with no evidence of any phase transitions to 7.8 GPa (Figs. 2 and 3). The fit of the P-V data yielded room pressure parameters V_0 = 425.667(20) Å^3,

FIGURE 1. Octahedral framework of stottite viewed down [001]. The FeO$_6$ octahedra are shaded dark gray and the GeO$_6$ octahedra are shaded light gray.

K_{T0} = 78.4(3) GPa, and K'_0 = 6.18(10) for the third-order Birch-Murnaghan equation of state. An f-F plot (Fig. 2b) provides visual confirmation that K'_0 is significantly greater than 4, similar in magnitude to orthorhombic perovskites (Ross and Angel 1999; Kung et al. 2001; Chaplin and Ross 2001). Fitting the data for any of these materials, including stottite, with a second-order EoS (i.e. K'_0 = 4) leads to significantly worse fits to the data and significant over-estimates of the bulk moduli.

The elastic moduli of the individual unit-cell axes of stottite were also obtained from the measured data by fitting a third-order Birch-Murnaghan equation of state to the cubes of each of the cell parameters in turn (Angel 2000). The resulting axial moduli (K_{d0}) and their pressure derivatives (K'_{d0}) are: K_{a0} = 81.3(3) GPa, K_{c0} = 73.3(6) GPa and K'_{a0} = 6.4(1), K'_{c0} = 5.7(2) (Fig. 3). The maximum anisotropy in the compressional moduli is thus about 10% with the shorter c dimension being more compressible than the longer a parameter.

DISCUSSION

Comparison with stottite-group minerals

The bulk modulus of 78.4(3) GPa obtained in this study for stottite, FeGe(OH)$_6$, is much higher than the bulk modulus of 44.7(9) GPa determined for burtite, CaSn(OH)$_6$ (Welch and Crichton 2002). The different compressibilities of Sn and Ge (and Ca and Fe^{2+}) octahedra are likely to be primarily responsible for the different compressibilities of the two minerals. However, hydrogen bonding may also have a measurable effect upon compressibility. The $a^+a^+c^-$ tilt system of stottite leads to a very different hydrogen-bonding topology from burtite, which has an $a^+a^+a^+$ tilt system. We will now examine the hydrogen-bonding topologies of stottite and burtite in some detail.

TABLE 1. Unit-cell parameters of stottite between 1 bar and 7.817 GPa

P(GPa)	a (Å)	c (Å)	V(Å^3)
0.0001	7.55041(9)	7.4664(4)	425.65(2)
0.671(3)	7.53043(10)	7.4446(4)	422.16(3)
1.471(5)	7.50785(11)	7.4195(5)	418.22(3)
2.331(4)	7.48442(9)	7.3937(4)	414.17(2)
3.702(4)	7.45020(10)	7.3561(4)	408.31(3)
4.022(5)	7.44256(9)	7.3487(4)	407.06(2)
4.788(6)	7.42567(9)	7.3292(4)	404.14(2)
5.689(5)	7.40560(10)	7.3073(4)	400.75(2)
6.343(6)	7.39196(8)	7.2924(3)	398.46(2)
7.284(7)	7.37329(10)	7.2717(4)	395.33(2)
7.817(8)	7.36266(12)	7.2604(5)	393.58(3)

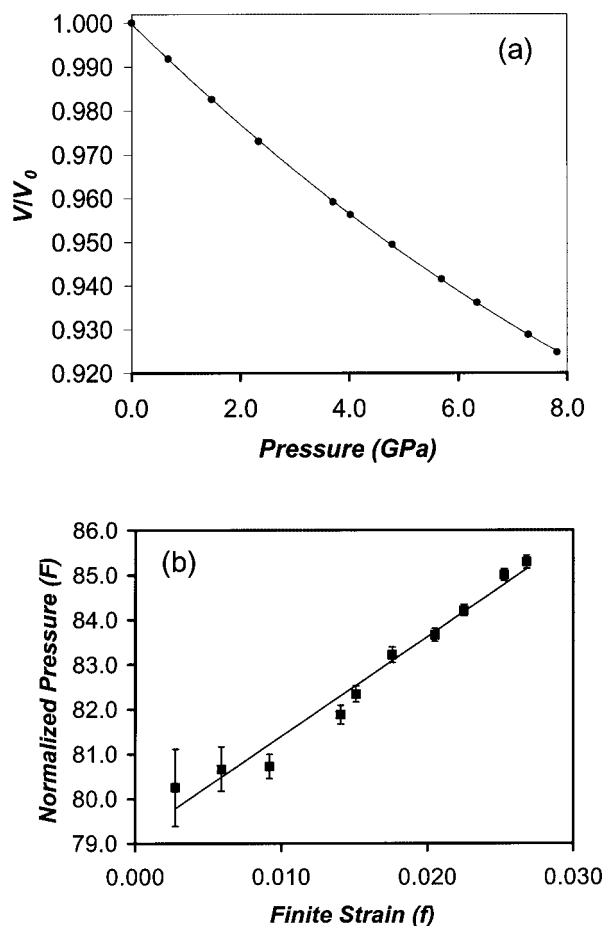*Note:* The figures in parentheses represent 1 e.s.d. of the last decimal place shown.

FIGURE 2. (a) Variation of volume of stottite with pressure at room temperature and (b) normalized stress-strain (F-f) plots derived from the measured volumes for a Birch-Murnaghan EoS. The lines are the equations of state fitted to the data, with the parameters given in the text.
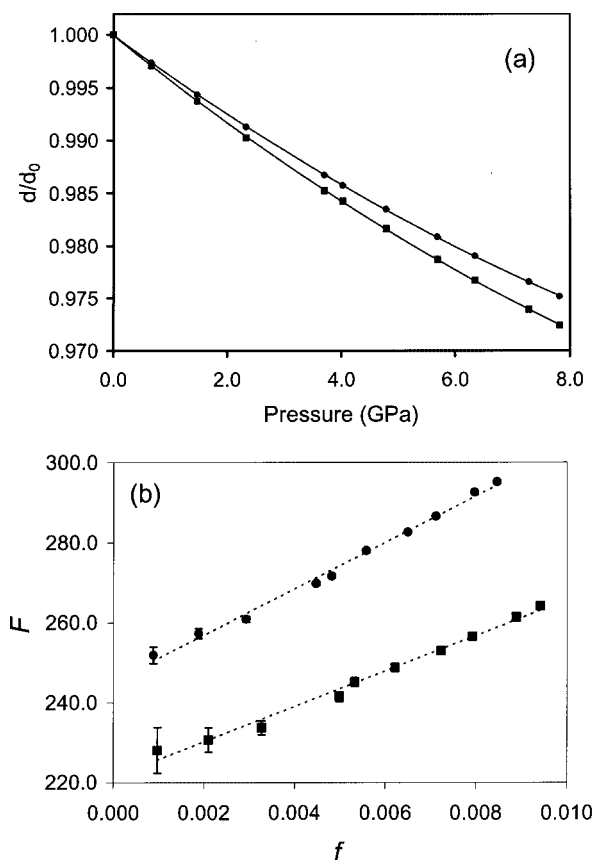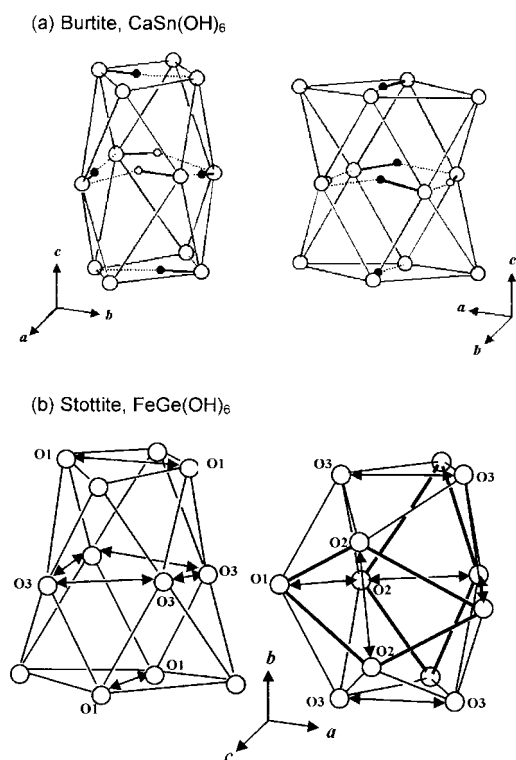

FIGURE 3. (a) Variation of a-axis (circles) and c-axis (squares) of stottite from 1 bar to 7.8 GPa and (b) normalized stress-strain (F-f) plots derived from the measured unit-cell data for a Birch-Murnaghan EoS. The lines are the equations of state fitted to the unit-cell data, with the parameters given in the text.

The cavity sites in stottite-group minerals are based upon a prismatically distorted cubo-octahedron. The cavities in burtite, $CaSn(OH)_6$, and stottite, $FeGe(OH)_6$ are shown in Figure 4. Burtite has a single type of cavity site whereas stottite has two very different cavity sites. Schoenfliesite, $MgSn(OH)_6$, has a cavity similar to burtite. The Mg and Sn octahedra are of very similar sizes (Mg-O = 2.11 Å, Sn-O = 2.05 Å), leading to a single cavity, which is almost undistorted (Basciano et al. 1998). Stottite, on the other hand, has two very different cavity sites, one of which is highly distorted. The distortion arises from the small size of the Ge octahedron coupled with the size difference between Fe and Ge octahedra (Ge-O ~ 1.91 Å, Fe-O ~ 2.16 Å). In burtite and schoenfliesite, six O-H···O linkages brace the cavity walls across the obtuse angles (short O-O distances): there is an equatorial ring of four hydrogen-bonded linkages and two further linkages, one at the top and one at the bottom of the cavity (Basciano et al. 1998). It is evident from Figure 4 that one cavity site in stottite is similar to that in burtite and can therefore be expected to have an equatorial ring of four O-H···O linkages (all O3-H···O3) and upper and lower O1-H···O1 linkages at the top and bottom of the cavity (although these are

perpendicular to each other, unlike in burtite where they are parallel). The other site is highly distorted and has the long and short O-O distances (O1-O1 and O2-O2, respectively) of two opposite quadrilateral cavity walls reversed ("occluded") compared with the regular arrangement shown by burtite. The O1-O1 distance of this site (4.67 Å) is far too long to allow an O-H···O linkage to form across it, and instead the missing linkage must occur across O2-O2 (2.70 Å).

Figure 5 shows the array of hydrogen-bonded linkages expected in stottite. These linkages correspond to the shortest O-O distance across each quadrilateral wall face, approximately bisecting the obtuse angle of the face. The array has two very different components: (1) rings of four O-H···O linkages (O3-H···O3) as in burtite, and (2) rows of <100> crankshafts of O1-H···O1, O1-H···O2, and O2-H···O2 linkages alternating in this sequence. Thus, there is greater hydrogen-bonded connectivity and continuity within the (001) plane than perpendicular to it. In fact, there is no hydrogen-bonded connectivity parallel to the **c**-axis. The O3 quartets occur in (002) layers. The higher compressibility of **c** compared with **a** observed in stottite may, therefore, be due to the considerably reduced hydrogen-bonding connectivity perpendicular to the (001) plane.
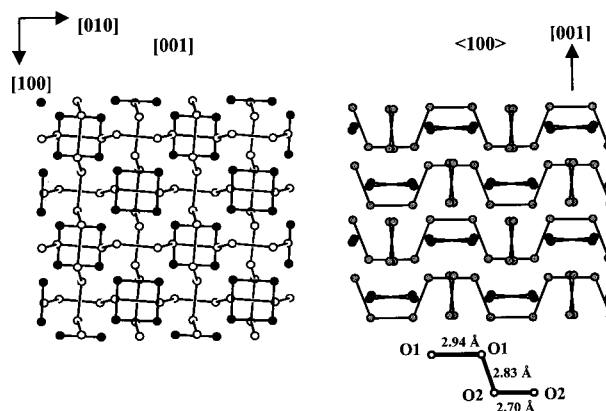
FIGURE 4. The cavity sites of (**a**) burtite and (**b**) stottite. The two upper figures show the same site in burtite viewed from two directions. The two lower figures show the burtite-like cavity in stottite (left) and the highly distorted cavity (right). O-H···O linkages for burtite and their analogous positions in stottite are indicated by double-headed arrows across the short O-O distances. The pair of "occluded" opposed quadrilateral cavity walls in stottite is shown by bold lines.

Comparison with related perovskites

It is also of interest to compare the bulk modulus of stottite with those of related perovskites in order to gain insight into how substitution of different octahedral framework cations and the presence of the non-framework cation affects the bulk modulus. Ross and Angel (1999) measured the equation of state (EoS) of $CaGeO_3$, a perovskite with a GeO_6 octahedral framework, and Chaplin and Ross (2001) measured the EoS of $GdFeO_3$, a perovskite with an $Fe^{3+}O_6$ octahedral framework. A third-order Birch-Murnaghan EoS fit to pressure-volume data measured by means of single-crystal X-ray diffraction measurements resulted in $K_{T0} = 194(2)$ GPa and $K_0' = 6.1(5)$ for $CaGeO_3$ (Ross and Angel 1999), and $K_{T0} = 182.9(9)$ GPa and $K_0' = 6.2(2)$ for $GdFeO_3$ (Chaplin and Ross 2001). Both structures are considerably less compressible than stottite, $FeGe(OH)_6$. Although hydrogen-bonding may play a secondary role in the compressibilities of protonated octahedral frameworks such as stottite compared with non-protonated perovskites, we believe that the major difference is due to the presence of a non-framework cation in perovskites, as discussed in more detail below.
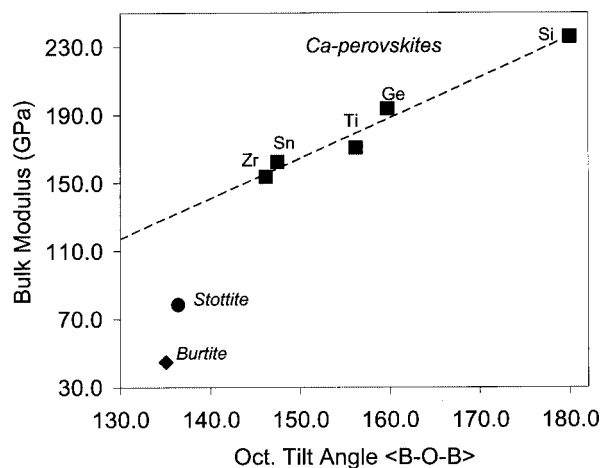
The tilt angles between octahedra in orthorhombic, oxide perovskites are generally larger than the octahedral tilt angles in protonated octahedral framework structures. The tilt angle between the CaO_6 and SnO_6 octahedra in burtite, for example,

FIGURE 5. The inferred hydrogen-bonded connectivity of stottite. Left is an [001] view showing the rows of <100> O-(H···)O crankshafts and the isolated four-membered rings. Right is a <100> view of the same structure in which the crankshafts are more clearly seen. The four-membered rings are seen on edge and lie in (002) layers.

is 135.05° (Basciano et al. 1998), 10° smaller than the tilt angle between ZrO_6 octahedra of $CaZrO_3$ perovskite, one of the most distorted of the Ca-oxide perovskites. As shown in Figure 6, the bulk moduli of the Ca-perovskites with different framework cations decrease systematically with increased tilting between the octahedra. Ca-perovskites with greater distortions from the ideal cubic symmetry (i.e., smaller <B-O-B> angles) have smaller bulk moduli and hence "softer" structures. The K_{T0} of burtite, 44.7(9) GPa (Welch and Crichton 2002), is much lower than $K_{T0} = 129$ GPa for a hypothetical Ca-perovskite with the same tilt angle predicted from the trend in Figure 6. Similarly, the <Fe-O-Ge> tilt angle in stottite, 136.4° (Ross II et al. 1988), is smaller than either the <Ge-O-Ge> tilt angle in $CaGeO_3$ perovskite, 159.7° (Sasaki et al. 1983), or the <Fe-O-Fe> tilt angle in $GdFeO_3$ perovskite, 147.1° (Marezio et al. 1970), although the latter has an $Fe^{3+}O_6$ framework. The K_{T0} of stottite, 78.4(3) GPa, is again much lower than that for a hypothetical Ca-perovskite with <B-O-B> = 136.4° predicted from the trend shown in Figure 6 ($K_{T0} = 133$ GPa). It is also much lower than the bulk modulus of brownmillerite, $Ca_2Fe_2O_5$, a defect perovskite, which has $K_{T0} = 127.0(5)$ GPa (Ross et al. 2002). We conclude that the absence of a non-framework cation is the main explanation why protonated octahedral frameworks are so much more compressible than the perovskite structures.

In perovskites, unit-cell compression is effected by two mechanisms: rigid rotations of octahedra and/or octahedral compression (e.g., Ross 2000). It has been shown that Ca-perovskites with greater distortions from ideal cubic symmetry display bulk moduli that lie above the linear trend between bulk modulus and density (Kung et al. 2001). This anomalous stiffening may be due to the structure reaching a "collapsibility limit" imposed by electrostatic repulsions between framework and non-framework cations, similar to what is observed in some tetrahedral framework structures (e.g., Baur 1992). Given the topological similarities between perovskite and stottite structures, combined with the absence of non-frame-

FIGURE 6. Plot of the bulk modulus as a function of octahedral tilt angle, comparing stottite with different framework cations in Ca-perovskites. Sources of EoS data: CaZrO$_3$ (Ross, unpublished data), CaSnO$_3$ (Kung et al. 2001), CaTiO$_3$ and CaGeO$_3$ (Ross and Angel 1999) and CaSiO$_3$ (Shim et al. 2000).

work cations, one might expect rigid rotations to play a key role in compression of stottite. On the other hand, considering the large tilt angles between the octahedra, one might also expect stottite to reach a "collapsibility limit" at high pressure and bond compression to dominate. A differential compressibility between the Fe- and Ge-octahedra would further drive the structure to becoming less anisotropic and more cubic at higher pressures. Research is underway to determine which compression mechanism(s) are operative in stottite at high pressure. The relative importance of an empty cavity site vs. the role of hydrogen bonding is likely to be a major issue in understanding the compressional behavior of protonated octahedral frameworks.

ACKNOWLEDGMENTS

REFERENCES CITED

Allan, D.R., Miletich, R., and Angel, R.J. (1996) A diamond-anvil cell for single-crystal X-ray diffraction studies to pressures in excess of 10 GPa . Reviews of Scientific Instruments, 67, 840–842.

Angel, R.J. (2000) Equations of state. In Hazen, R.M., Downs, R.T., Eds., High-temperature and high-pressure crystal chemistry. Reviews in Mineralogy and Geochemistry, 41, p. 35–60. Mineralogical Society of America, Washington, D.C.

Angel, R.J., Allan, D.R., Miletich, R., and Finger, L.W. (1997) The use of quartz as an internal pressure standard in high-pressure crystallography. Journal of Applied Crystallography, 30, 461–466.

Angel, R.J., Downs, R.T., and Finger, L.W. (2000) High-temperature, high-pressure diffractometry. In Hazen, R.M., Downs, R.T., Eds., High-pressure and high-temperature crystal chemistry, 41, p. 559–596. Reviews in Mineralogy and Geochemistry, Mineralogical Society of America, Washington, D.C.

Basciano, L.C., Peterson, R.C., Roeder, P.L., and Swainson, I. (1998) Description of schoenfliesite, MgSn(OH)$_6$, and roxbyite, Cu$_{1.72}$S, from a 1375 BC shipwreck, and Rietveld neutron-diffraction refinement of synthetic schoenfliesite,

wickmannite, MnSn(OH)$_6$, and burtite, CaSn(OH)$_6$. Canadian Mineralogist, 36, 1203–1210.

Baur, W.H. (1992) Self-limiting distortion by anti-rotating hinges is the principle of flexible but non-collapsible frameworks. Journal of Solid State Chemistry 97, 243–247.

Bernstein, L.R. and Waychunas, G.A. (1987) Germanium crystal chemistry in hematite and goethite from the Apex mine, Utah, and some new data on germanium in aqueous solution and in stottite. Geochimica et Cosmochimica Acta, 51, 623–630.

Birch, F. (1947) Finite elastic strain of cubic crystals. Physical Review, 71, 809–824.

Chaplin, T.D. and Ross, N.L. (2001) Effect of Al/Fe substitution on the bulk moduli of GdAlO$_3$ and GdFeO$_3$ perovskites. EOS, Transactions of the American Geophysical Union, 82, S416.

Cohen-Addad, C. (1968) Étude structurale des hydroxystannates CaSn(OH)$_6$ et ZnSn(OH)$_6$ par diffraction neutronique, absorption infrarouge et résonance magnétique nucléaire. Bulletin de la Societe francaise de Minéralogie et de Cristallographie, 91, 315–324.

Faust, G.T. and Scaller, W.T. (1971) Schoenfliesite, MgSn(OH)6. Zeitschrift für Kristallographie, 116–141.

Glazer, A.M. (1972) The classification of tilted octahedra in perovskites. Acta Crystallographica, B28, 3384–3392.

Kampf, A.R. (1982) Jeanbandyite, a new member of the stottite group from Llallagua, Bolivia. Mineralogical Record, 12, 235–239.

King, H.E. and Finger, L.W. (1979) Diffracted beam crystal centering and its application to high pressure crystallography. Journal of Applied Crystallography, 12, 374–378.

Kung, J., Angel, R.J., and Ross, N.L. (2001) Elasticity of CaSnO$_3$ perovskite. Physics and Chemistry of Minerals, 28, 35–43.

Marezio, M., Remeika, J.P., and Dernier, P.D. (1970) The crystal chemistry of the rare earth orthoferrites. Acta Crystallographica, B26, 2008–2022.

Moore, P.B. and Smith, J.V. (1967) Wickmanite, Mn^{+2}[Sn^{4+}(OH)$_6$], a new mineral from Långban. Arkiv for Mineralogi och Geologi, 4, 395–399.

O'Keeffe, M. and Hyde, B.G. (1977) Some structures topologically related to cubic perovskite (E2$_1$), ReO$_3$ (DO$_9$) and Cu$_3$Au (L1$_2$). Acta Crystallographica, B33, 3802–3813.

Orear, J. (1982) Least squares when both variables have uncertainties. American Journal of Physics, 50, 912–916.

Ralph, R.L. and Finger, L.W. (1982) A computer program for refinement of crystal orientation matrix and lattice constants from diffractometer data with lattice constraints. Journal of Applied Crystallography, 15, 537–539.

Ross II, C., Bernstein, L.R., and Waychunas, G.A. (1988) Crystal-structure refinement of stottite, FeGe(OH)$_6$. American Mineralogist, 73, 657–661.

Ross, N.L. (2000) Framework structures. In R.M. Hazen and R.T. Downs, Eds., High-temperature and high-pressure crystal chemistry. Reviews in Mineralogy and Geochemistry, 41, p. 257–288. Mineralogical Society of America, Washington, D.C.

Ross, N.L. and Angel, R.J. (1999) Compression of CaTiO$_3$ and CaGeO$_3$ perovskites. American Mineralogist, 84, 277–281.

Ross, N.L., Angel, R.J., and Seifert, F. (2002) Compressibility of Brownmillerite, Ca$_2$Fe$_2$O$_5$: Effect of vacancies on the elastic properties of perovskites. Physics of the Earth and Planetary Interiors, 129, 145–151.

Sasaki, S., Prewitt, C.T., and Libermann, R.C. (1983) The crystal structure of CaGeO$_3$ perovskite and the crystal chemistry of the GdFeO$_3$-type perovskites. American Mineralogist, 68, 1189–1198.

Shim, S.H., Duffy, T.S., and Shen, G.Y. (2000) The equation of state of CaSiO$_3$ perovskite to 108 GPa at 300 K. Physics of Earth and Planetary Interiors, 120, 327–338.

Sonnet, P.B. (1981) Burtite, calcium hexahydroxystannate, a new mineral from El Hamman, central Morocco. Canadian Mineralogist, 19, 397–401.

Strunz, H. and Giglio, M. (1961) Die Kristallstruktur von Stottit, Fe[Ge(OH)$_6$]. Acta Crystallographica, 14, 205–208.

Strunz, H., Sohnge, G., and Geier, B.H. (1958) Stottit, ein neues Germanium-Mineral und seine Paragenese in Tsumeb. Neues Jahrbuch für Mineralogie Monatshefte, 85–96.

Welch, M.D. and Crichton, W.A. (2002) Compressibility to 7 GPa of the protonated octahedral framework mineral burtite, CaSn(OH)$_6$. Mineralogical Magazine, 66, 431–440.

Zemann, J. (1959) Der Strukturtyp von Stottit. Neues Jahrbuch für Mineralogie Monatshefte, 67–69.